EMi | Taylor & Francis
Taylor & Francis Group

RESEARCH ARTICLE

OPEN ACCESS  Check for updates

# SARS-CoV-2 pseudovirus enters the host cells through spike protein-CD147 in an Arf6-dependent manner

Yun-Qi Zhou[a,b]†, Ke Wang[b]†, Xue-Yan Wang[a,b], Hong-Yong Cui[b], Yongxiang Zhao[a], Ping Zhu[c] and Zhi-Nan Chen[a,b]

[a]National Center for International Research of Bio-targeting Theranostics, Guangxi Key Laboratory of Bio-targeting Theranostics, Collaborative Innovation Center for Targeting Tumor Diagnosis and Therapy, Guangxi Talent Highland of Bio-targeting Theranostics, Guangxi Medical University, Nanning, People's Republic of China; [b]National Translational Science Center for Molecular Medicine & Department of Cell Biology, Fourth Military Medical University, Xi'an, People's Republic of China; [c]Department of Clinical Immunology, Xijing Hospital, Fourth Military Medical University, Xi'an, People's Republic of China

**ABSTRACT**
The spread of severe acute respiratory syndrome coronavirus 2 (SARS-CoV-2) and its variants is threatening public health around the world. Endocytosis functions as an important way for viral infection, and SARS-CoV-2 bears no exception. However, the specific endocytic mechanism of SARS-CoV-2 remains unknown. In this study, we used endocytic inhibitors to evaluate the role of different endocytic routes in SARS-CoV-2 pseudovirus infection and found that the viral infection was associated with caveolar/lipid raft- and cytoskeleton-mediated endocytosis, but independent of the clathrin-mediated endocytosis and macropinocytosis. Meanwhile, the knockdown of CD147 and Rab5a in Vero E6 and Huh-7 cells inhibited SARS-CoV-2 pseudovirus infection, and the co-localization of spike protein, CD147, and Rab5a was observed in pseudovirus-infected Vero E6 cells, which was weakened by CD147 silencing, illustrating that SARS-CoV-2 pseudovirus entered the host cells via CD147-mediated endocytosis. Additionally, Arf6 silencing markedly inhibited pseudovirus infection in Vero E6 and Huh-7 cells, while little change was observed in CD147 knockout-Vero E6 cells. This finding indicated Arf6-mediated CD147 trafficking plays a vital role in SARS-CoV-2 entry. Taken together, our findings provide new insights into the CD147-Arf6 axis in mediating SARS-CoV-2 pseudovirus entry into the host cells, and further suggest that blockade of this pathway seems to be a feasible approach to prevent the SARS-CoV-2 infection clinically.

## Introduction

Coronavirus disease 2019 (COVID-19) caused by SARS-CoV-2 has given rise to a global pandemic, which brought serious harm to human health. The emergence of variants, such as delta and omicron, enhances viral transmission and immune escape, posing a huge challenge to overcome the epidemic [1,2]. Therefore, it is indispensable to elucidate the mechanism of virus infection, providing a theoretical basis for treating COVID-19.

It has been reported that the entry modes of most viruses involve membrane fusion and endocytosis, which are the key steps for viral propagation [3].

The process of membrane fusion is initiated by fusion peptides, which then allow the release of the viral genome in the host cells [4]. Angiotensin-converting enzyme 2 (ACE2) is a vital cell-surface receptor for SARS-CoV-2 infection via membrane fusion [5]. The S1 subunit of spike protein serves the function of binding to ACE2, followed by the fusion of the virus and cell membrane to release the virus genome into the cell, which is mediated by the S2 subunit of spike protein [6,7]. Endocytosis is an important entry mode for virus infection. Most viruses depend on endocytic uptake, vesicular transport, and delivery to intracellular organelles. The main types of endocytosis contain clathrin-mediated endocytosis, caveolar/lipid

raft-mediated endocytosis, macropinocytosis, Arf6-dependent endocytosis, and flotillin-dependent endocytosis [8,9]. Numerous viruses employ multiple endocytic pathways to infect the host cells [10–12]. As for SARS-CoV-2, endocytosis plays an essential role in virus infection.

Our previous study showed that CD147 is a novel receptor for SARS-CoV-2 infection, and SARS-CoV-2 enters the host cells through CD147-mediated endocytosis [13]. However, the mechanism of CD147-mediated viral endocytosis is still unclear. CD147 is a type I transmembrane glycoprotein (also known as basigin, M6, or EMMPRIN [14–16]), which is closely involved in tumor progression, inflammatory response, plasmodium invasion, and viral infection [13,17–21]. The internalization of CD147 depends on clathrin-independent endocytosis, which is closely related to ADP-ribosylation factor 6 (Arf6), a master regulator of membrane trafficking [22]. Based on the above researches, there still exists a necessity to investigate the possible role of Arf6 in CD147-mediated SARS-CoV-2 infection.

In our study, we found that SARS-CoV-2 pseudovirus entry was related to caveolar/lipid raft- and cytoskeleton-mediated endocytosis. CD147 was an important receptor for SARS-CoV-2 pseudovirus entry, which was regulated by Arf6-dependent endocytosis. Our study gives new insights into the endocytic pathway of SARS-CoV-2, which contributes to understanding the process of the virus infection and provides a potential target for COVID-19 treatment.

## Materials and methods

### Cell lines

Vero E6 and Huh-7 cell lines were obtained from the Cell Bank of the Chinese Academy of Sciences (Shanghai, China) and the Japanese Collection of Research Bioresources (Osaka, Japan), respectively. CD147 knockout in Vero E6 cell (Vero E6-CD147KO) was constructed using a CRISPR/Cas9 gene editing system (GeneChem, China). All the cell lines were authenticated using a short tandem repeat DNA profiling (Beijing Microread Genetics, China), and were cultured in Dulbecco's modified eagle medium (DMEM) with 10% fetal bovine serum (FBS) and 2% L-glutamine at 37°C under 5% $CO_2$.

### SARS-CoV-2 pseudovirus

SARS-CoV-2 pseudovirus with luciferase [23] was obtained from the Institute for Biological Product Control, National Institutes for Food and Drug Control (Beijing, China).

### Inhibitors, antibodies, and reagents

Chemical inhibitors used in the study are listed as follows: chlorpromazine HCl (CPZ, S2456, Selleck), nocodazole (S2775, Selleck), 5-(N-ethyl-N-isopropyl) amiloride hydrochloride (EIPA, HY-101840A, Med Chem Express), methyl-β-cyclodextrin (MCD, HY-101461, Med Chem Express), cytochalasin D (Cyto D, HY-N6682, Med Chem Express), and filipin III (SAE0087, Sigma). CPZ and MCD were dissolved in water, and the others were dissolved in dimethyl sulfoxide to prepare master stocks for storage. Primary antibodies used in this study included rabbit anti-Arf6 antibody (PA1-093, Invitrogen), rabbit anti-Rab5a antibody (2143 T, Cell Signaling Technology), mouse anti-SARS-CoV-2 spike antibody (Sino Biological), and human anti-CD147 antibody (meplazumab, MPZ, Jiangsu Pacific Meinuoke Biopharmaceutical Co. Ltd), mouse anti-CD147 antibody (orb251620, Biorbyt), goat anti-ACE2 antibody (AF933, R&D Systems), mouse anti-tubulin antibody (66031-1-Ig, Proteintech). Goat anti-human IgG (H + L) cross-adsorbed secondary antibody, Alexa Fluor 647 (A21445, Invitrogen), donkey anti-mouse IgG (H + L) highly cross-adsorbed secondary antibody, Alexa Fluor 488 (A21202, Invitrogen), and donkey anti-rabbit IgG (H + L) highly cross-adsorbed secondary antibody, Alexa Fluor 555 (A31572, Invitrogen) were used in the immunofluorescence assay. Peroxidase-conjugated rabbit anti-goat IgG (H + L) (ZB-2306, ZSGB-Bio), goat anti-rabbit IgG (H + L) secondary antibody, HRP (31460, Invitrogen), and goat anti-mouse IgG (H + L) secondary antibody, HRP (31430, Invitrogen) were used in western blot analysis. The endocytic fluorescent markers were used in this study, including Alexa Fluor 555 dextran (D34679, Invitrogen), Alexa Fluor 555 transferrin from human serum (T35352, Invitrogen), Alexa Fluor 555 cholera toxin subunit B (CTB, C34776, Invitrogen), and Alexa Fluor 488 phalloidin (A12379, Invitrogen). Hoechst 33342 (C1022, Beyotime) and 2-(4-amidino-phenyl)-6-indolecarbamidine (DAPI, C1002, Beyotime) were used to stain the nuclei. Cell counting kit-8 (CCK-8, C0005, Topscience) and a dual-luciferase reporter assay system (E1980, Promega) were also used in the study.

### Cytotoxicity assay

Vero E6 cells were seeded in 96-well plates at 37°C overnight, and then, incubated with different concentrations of the inhibitors for 48 h. Subsequently, the supernatants were removed and the mixed solution (100μl DMEM plus 10 μl cell counting kit-8 (CCK-8) reagent) was added to each well. After incubating at 37°C for 1 h, the optical density (OD) value was

determined at 450 nm using a microplate reader (Bio-Tek Epoch).

## Cellular uptake assay

Vero E6 cells ($8 \times 10^4$ cells/dish) were cultured in a confocal dish overnight, and then, incubated with corresponding inhibitors in the DMEM (2% FBS) or DMEM (2% FBS) only for 24 h at 37°C. Next, the cells were kept on ice for 10 min and washed with a cold live cell imaging solution (LCIS, A14291DJ, Invitrogen) containing 20 mM glucose and 1% bovine serum albumin. After incubating with the endocytosis fluorescent markers (dextran, transferrin, and CTB) at 37°C for 2–4 h, the cells were washed with the LCIS, and Hoechst 33342 was used to stain the nuclei for 10 min. After being washed with the LCIS twice, the dishes were immediately observed to capture the images in a fluorescent microscope.

## Pseudovirus infection assay

Luciferase activity was determined using a luciferase assay kit (E1980, Promega). Vero E6 and Huh-7 cells ($10^4$ cells/well) were seeded in 96-well plates overnight at 37°C. The cell supernatants were removed and the mixed solution (100 µl DMEM plus 5 µl SARS-CoV-2 pseudovirus) was added to each well. After incubating at 37°C for 24 h, the cells were washed with PBS and lysed using a 50 µl passive lysis buffer with gentle rocking for 20 min at room temperature. Then, a 100 µl luciferase assay reagent II was added to each well, and the data were obtained from a luminometer (E5311, Promega). For the virus inhibition assay, the cells were incubated with corresponding inhibitors in the DMEM (2% FBS) for 24 h or were transfected with siRNAs before the virus infection.

## siRNA transfection

Gene silencing was conducted by transfecting siRNA (GenePharma) using a jetPRIME® transfection reagent (PT-114-15, Polyplus) according to the instructions of the manufacturer. The siRNA sequences for the targeted genes are listed as follows:

siCtrl sense: 5′-UUCUCCGAACGUGUCACGUTT-3′

siCtrl antisense: 5′-ACGUGACACGUUCGGA-GAATT-3′

siCD147 (green monkey) sense: 5′-GAACGA-CAAAGGCAAGAAATT-3′

siCD147 (green monkey) antisense: 5′-UUUCUUGC-CUUUGUCGUUCTT-3′

siArf6 (green monkey) sense: 5′-CCUCUAACUA-CAAAUCUUATT-3′

siArf6 (green monkey) antisense: 5′-UAAGAUUU-GUAGUUAGAGGTT-3′

siRab5a (green monkey) sense: 5′-GGGCCAAAUA-CUGGAAAUATT-3′

siRab5a (green monkey) antisense: 5′-UAUUUCCA-GUAUUUGGCCCTT-3′

siCD147 (human) sense: 5′-GACCUUGGCUCCAA-GAUACTT-3′

siCD147 (human) antisense: 5′-GUAUCUUGGAGC-CAAGGUCTT-3′

siArf6 (human) sense: 5′-CGGCAUUACUACA-CUGGGATT-3′

siArf6 (human) antisense: 5′-UCCCAGUGUA-GUAAUGCCGTT-3′

siRab5a (human) sense: 5′-GAGUCCGCUGUUGG-CAAAUCA-3′

siRab5a (human) antisense: 5′-UGAUUUGCCAA-CAGCGGACUC-3′

## Real-time PCR (RT–PCR)

Total RNA was extracted using the total RNA kit II (D6934-01, Omega Bio-Tek) and transcribed into cDNA using PrimeScript™ RT Master Mix (RR036A, Takara). RT–PCR was performed to detect the expression of target genes using TB Green® Premix Ex Taq™ II (RR820A, Takara). The sequences of corresponding primers were listed as follows:

Actin (green monkey) -Forward: 5′-GCCGTCTTCCCCTCCATCGT-3′

Actin (green monkey) -Reverse: 5′-TCTGGGTCATCTTCTCGCGG-3′

CD147 (green monkey) -Forward: 5′-GGCTCGAA-GACACTCCTCAC-3′

CD147 (green monkey) -Reverse: 5′-GAG-TACTCTCCCCCGAGGTC-3′

Arf6 (green monkey) -Forward: 5′-GCGGCATTAC-TACACTGGGA-3′

Arf6 (green monkey) -Reverse: 5′-CCCTCATCTCCCGGTCATTG-3′

Rab5a (green monkey) -Forward: 5′-GCTAATC-GAGGCGCAACAAG-3′

Rab5a (green monkey) -Reverse: 5′-GGTTA-GAAAAGCAGCCCCAA-3′

ACE2 (green monkey) -Forward: 5′- GTGCA-CAAAGGTGACAATGG-3′

ACE2 (green monkey) -Reverse: 5′- GGCTGCA-GAAAGTGACATGA-3′

Actin (human) -Forward: 5′-CATGTACGTTGC-TATCCAGGC-3′

Actin (human) -Reverse: 5′-CTCCTTAATGTCACG-CACGAT-3′

CD147 (human) -Forward: 5′-GACGACCAGTGGG-GAGAGTA-3′

CD147 (human) -Reverse: 5′-GGCCTTGTCCTCA-GAGTCAG-3′

Arf6 (human) -Forward: 5′-CCCAAGGTCT-CATCTTCGTAGT-3′

Arf6 (human) -Reverse: 5′-GTGGGGTTTCATGG-CATCG-3′

Rab5a (human) -Forward: 5′-AGACCCAACGGGC-CAAATAC-3′

Rab5a (human) -Reverse: 5′-GCCCCAATGG-TACTCTCTTGAA-3′

## Western blot analysis

To obtain the protein samples, the cells were collected, washed with PBS, and lysed in the RIPA lysis buffer (P0013B, Beyotime) supplemented with phenylmetha-nesulfonyl fluoride (PMSF, ST505, Beyotime). The protein concentrations were determined by a BCA protein assay kit (P0011, Beyotime); then the lysate was mixed with a 5× loading buffer and heated for 10 min at 100°C. The protein samples were loaded onto 10% SDS-PAGE and transferred to the PVDF membranes (IPVH00010, Millipore). After being blocked with 5% skimmed milk in the TBST buffer for 1 h, the PVDF membranes were incubated with specific primary antibodies (rabbit anti-Arf6 antibody, PA1-093, Invitrogen; rabbit anti-Rab5a antibody, 2143T, cell signaling technology; mouse anti-CD147 antibody, orb251620, Biorbyt; goat anti-ACE2 antibody, AF933, R&D Systems; mouse anti-tubulin antibody, 66031-1-Ig, Proteintech) at 4°C overnight. Next, the membranes were incubated with horseradish peroxidase-conjugated secondary antibodies (peroxidase-conjugated rabbit anti-goat IgG (H + L), ZB-2306, ZSGB-Bio; goat anti-rabbit IgG (H + L) secondary antibody, HRP, 31460, Invitrogen; goat anti-mouse IgG (H + L) secondary antibody, HRP, 31430, Invitrogen) for 1 h at room temperature and the images were obtained and analyzed using the Image Lab software (BIO-RAD).

## Immunofluorescence staining

The cells were cultured in confocal dishes overnight at 37°C, and then, incubated with a 2% FBS DMEM with 30μl SARS-CoV-2 pseudovirus or a 2% FBS DMEM only for 24 h. Next, the cells were fixed with 4% paraformaldehyde fix solution (AR1069, Boster) for 15 min and permeabilized with 0.02% Triton X-100 (A600198-0500, BBI Life Sciences) for 3 min, followed by incubation with 5% goat serum for 1 h. Subsequently, the cells were incubated with the corresponding primary antibodies (rabbit anti-Arf6 antibody, PA1-093, Invitrogen; rabbit anti-Rab5a antibody, 2143T, cell signaling technology; mouse anti-SARS-CoV-2 spike antibody, Sino Biological; human anti-CD147 antibody, MPZ, Jiangsu Pacific Meinuoke Biopharmaceutical Co. Ltd) overnight at 4°C. After

being washed three times with PBS, the cells were stained with corresponding immunofluorescent secondary antibodies (goat anti-human IgG (H + L) cross-adsorbed secondary antibody, Alexa Fluor 647, A21445, Invitrogen, donkey anti-mouse IgG (H + L) highly cross-adsorbed secondary antibody, Alexa Fluor 488, A21202, Invitrogen, donkey anti-rabbit IgG (H + L) highly cross-adsorbed secondary antibody, Alexa Fluor 555, A31572, Invitrogen) for 1 h at room temperature, and DAPI was used to stain the nuclei for 10 min. The images were collected using confocal laser scanning microscopy.

## Statistical analysis

All statistical data were performed using the Graph-Pad Prism V8.0. These experiments were performed in triplicate. Statistical analyses were performed using a student's t-test or student's t-test with Welch's correction. $P < 0.05$ was considered to be a significant difference.

## Results

### SARS-CoV-2 pseudovirus enters the host cells through CD147-mediated endocytosis

Our previous study showed that CD147 is a vital receptor for SARS-CoV-2 infection, which facilitates viral entry through endocytosis [13]. In our study, a pseudovirus infection assay was performed using CD147 silencing cells and the result showed that the knockdown of CD147 in Vero E6 and Huh-7 cells significantly inhibited pseudovirus infection (Figure 1A, B). Vero E6-CD147KO cell line was also constructed using a CRISPR-Cas9 system and a similar finding was obtained in the pseudovirus infection assay (Figure 1C). Rab5a is located in the plasma membrane and early endosomes, which functions as a key regulatory molecule for vesicle transport during early endocytosis [24–26]. To investigate the role of Rab5a in SARS-CoV-2 pseudovirus entry, Rab5a knockdown-Vero E6 and Huh-7 cells were constructed and the pseudovirus infection assay that demonstrated Rab5a silencing in these cells markedly attenuated viral infection (Figure 1D, E). We also found that the silencing of CD147 or Rab5a in Vero E6 cells has no impact on the expression of ACE2 in the mRNA and protein levels (Sup. Figure 1A-D). Meanwhile, immunofluorescence staining showed the co-localization of CD147 and Rab5a in Vero E6 cells (Figure 1F), as well as the silencing of CD147 in Vero E6 and Huh-7 cells, which decreased the expression of Rab5a using RT–PCR (Figure 1G, H). To confirm CD147-mediated SARS-CoV-2 endocytosis, immunofluorescence staining was performed using confocal microscopy to detect the localization
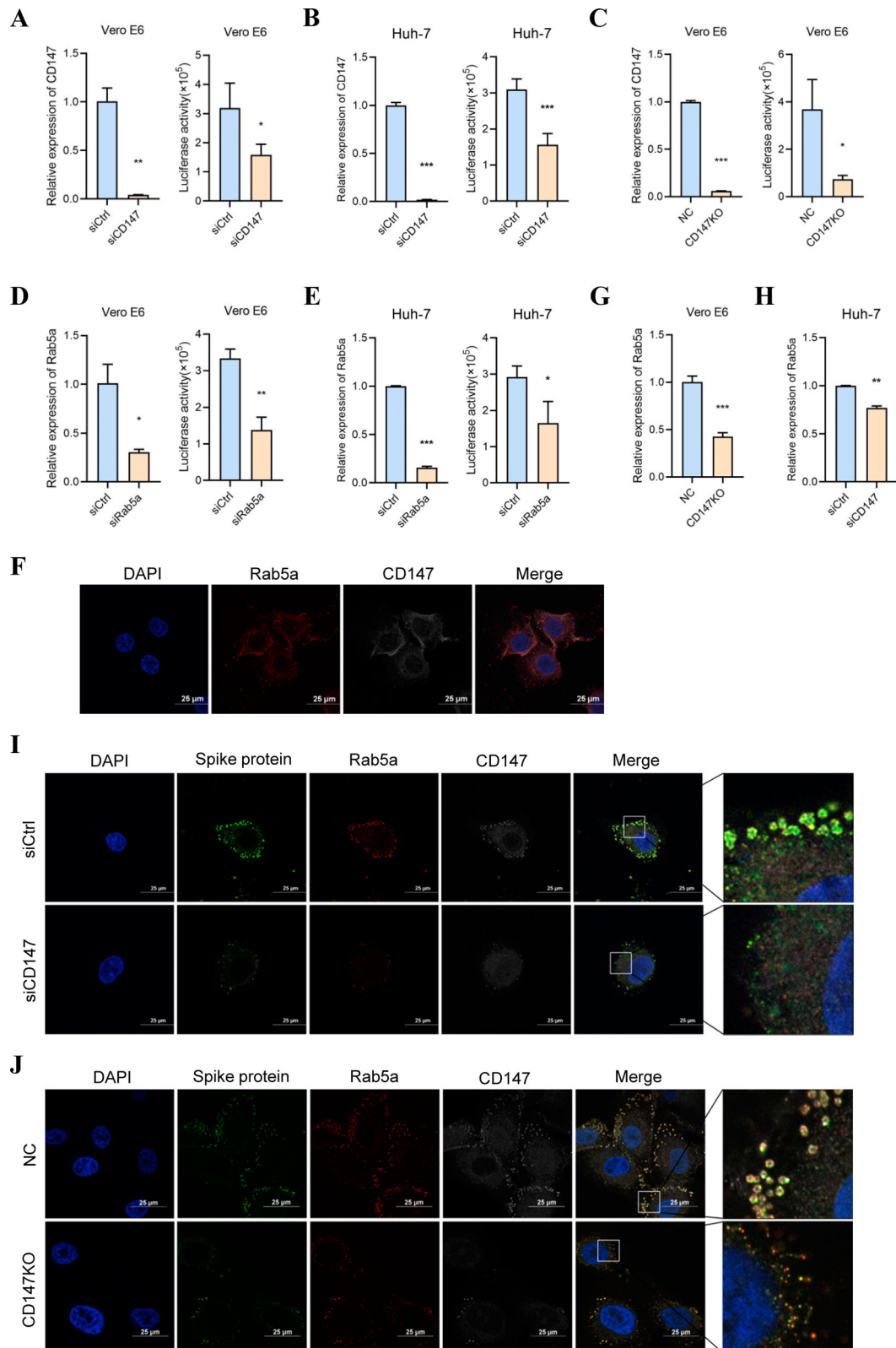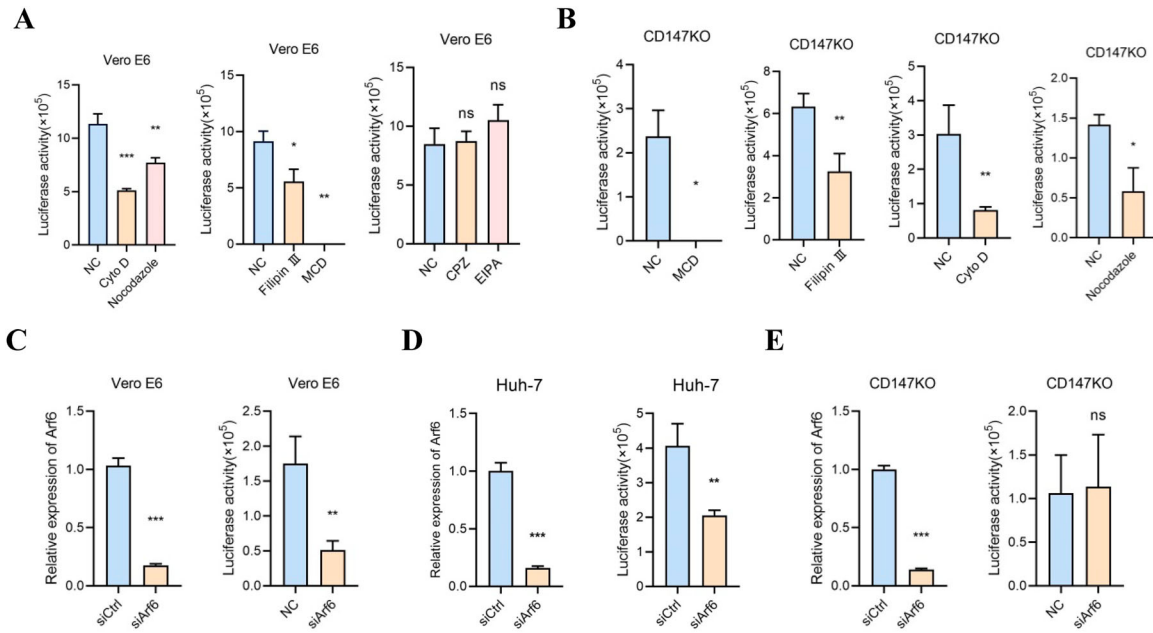
**Figure 1.** SARS-CoV-2 pseudovirus enters the host cells through CD147-mediated endocytosis. (A–C) Left, the knockdown or knockout of CD147 in Vero E6 and Huh-7 cells was detected by RT-PCR (**$P < 0.01$, ***$P < 0.001$). Right, SARS-CoV-2 pseudovirus infection in different cells was performed by the luciferase reporter assay (*$P < 0.05$, ***$P < 0.001$). (D, E) Left, Rab5a knockdown in Vero E6 and Huh-7 cells was detected by RT-PCR (*$P < 0.05$, ***$P < 0.001$). Right, SARS-CoV-2 pseudovirus infection in siRab5a cells and the control cells was performed by luciferase reporter assay (*$P < 0.05$, **$P < 0.01$). (F) The co-localization between Rab5a (red) and CD147 (white) was analyzed in Vero E6 cells by immunofluorescence staining. Scale bars, 25 μm. (G, H) Relative Rab5a mRNA level was detected by RT-PCR in the control and Vero E6-CD147KO or Huh-7-siCD147 cells (**$P < 0.01$, ***$P < 0.001$). (I, J) The co-localization of spike protein (green), Rab5a (red), and CD147 (white) were analyzed in Vero E6 cells and CD147 silencing cells by multicolour immunofluorescence staining. Scale bars, 25 μm.
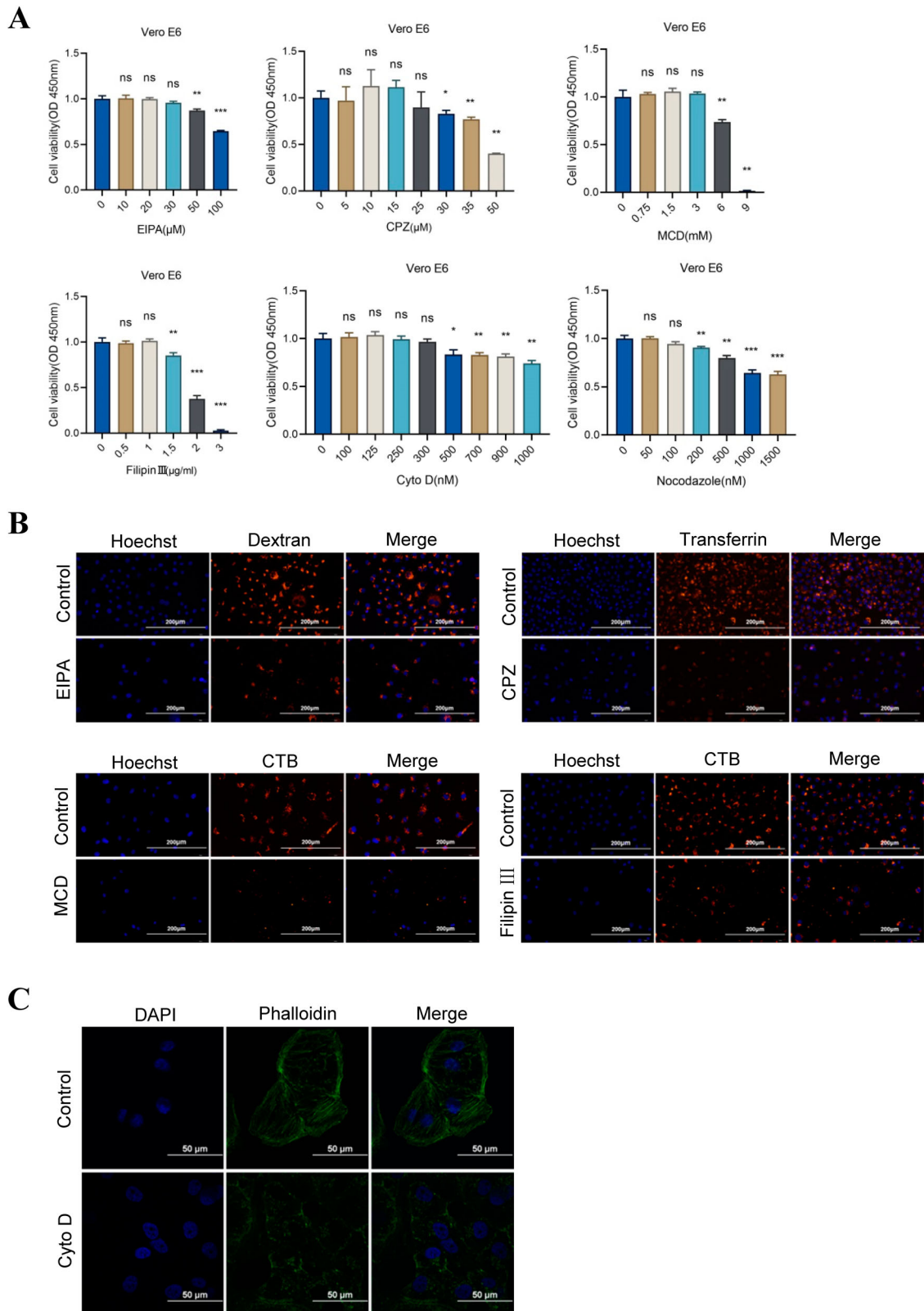
**Figure 2.** The screening for appropriate concentrations of different inhibitors. (A) Cell cytotoxicity was detected under different concentrations of inhibitors by the CCK-8 assay (*$P < 0.05$, **$P < 0.01$, ***$P < 0.001$, ns, not significant). (B) The blocking effect of EIPA (30 μM) on dextran, CPZ (25 μM) on transferrin, and MCD (3 mM) or filipin III (1 μg/ml) on CTB was observed in Vero E6 cells. Hoechst was used to stain the nuclei. Scale bars, 200 μm. (C) Phalloidin was used to evaluate the effect of cyto D (300 nM) on disrupting actin polymerization. Scale bars, 50 μm.

of the SARS-CoV-2 spike protein, CD147, and Rab5a. As shown in Figure 1I, J, a strong co-localization among spike protein (green), Rab5a (red), and CD147 (white), characterized a punctate pattern and was observed surrounding the cytoplasm near the membrane regions of Vero E6 cells, while a weakened signal of CD147 (white), Rab5a (red) and spike protein (green) was observed in the CD147 silencing cells.

**Figure 3.** SARS-CoV-2 pseudovirus enters the host cells through spike protein-CD147 in an Arf6-dependent manner. (A) Vero E6 cells were pretreated with six inhibitors, respectively, for 24 h, and incubated with SARS-CoV-2 pseudovirus. The SARS-CoV-2 pseudovirus infection in the different groups was detected by the luciferase reporter assay (*$P < 0.05$, **$P < 0.01$, ***$P < 0.001$, ns, not significant). (B) Vero E6-CD147KO cells were pretreated with four inhibitors (MCD, filipin III, cyto D, and nocodazole) respectively for 24 h, and incubated with SARS-CoV-2 pseudovirus. The SARS-CoV-2 pseudovirus infection in the different groups was detected by the luciferase reporter assay (*$P < 0.05$, **$P < 0.01$). (C-E) Left, the knockdown of Arf6 in Vero E6, Huh-7, and Vero E6-CD147KO cells was detected by RT-PCR (***$P < 0.001$). Right, SARS-CoV-2 pseudovirus infection in different cells was performed by the luciferase reporter assay (**$P < 0.01$, ns, not significant).

These results further indicated that the deficiency of CD147 prevented the entry of SARS-CoV-2 pseudovirus and Rab5a expression. Our findings show that SARS-CoV-2 pseudovirus enters the host cells through CD147-mediated endocytosis.

## SARS-CoV-2 pseudovirus enters the host cells through spike protein-CD147 in an Arf6-dependent manner

It has been reported that the main types of endocytosis for virus infection contain clathrin-mediated endocytosis, caveolar/lipid raft-mediated endocytosis, and macropinocytosis [8,9]. To clarify the endocytic mechanisms of SARS-CoV-2 entry, some inhibitors of endocytic routes were used to perform the virus inhibitory assays, including EIPA (an inhibitor of macropinocytosis), CPZ (an inhibitor of clathrin-mediated endocytosis), cyto D (an inhibitor of actin polymerization), nocodazole (depolymerizing microtubules), MCD, and filipin III (inhibitors of caveolar/lipid raft-mediated endocytosis). Primarily, cell cytotoxicity was conducted to screen appropriate working concentrations of pharmacologic inhibitors by the CCK-8 assay. According to the methods adopted in previous study, the concentration of EIPA (10, 20, 30, 50, 100 μM), CPZ (5, 10, 15, 25, 30, 35, 50 μM), MCD (0.75, 1.5, 3, 6, 9 mM), filipin III (0.5, 1, 1.5, 2, 3 μg/ml), cyto D (100, 125, 250, 300, 500, 700, 900, 1000 nM), and nocodazole (50,

100, 200, 500, 1000, 1500 nM) were set up. Cell cytotoxicity showed that the optimal concentration of EIPA, CPZ, MCD, filipin III, cyto D, and nocodazole were 30 μM, 25 μM, 3 mM, 1 μg/ml, 300 nM, and 100 nM, respectively (Figure 2A). To verify the inhibitory effect of these inhibitors under the selected concentrations, dextran (an endocytic marker for macropinocytosis), transferrin (a marker for clathrin-mediated endocytosis), and CTB (a marker for caveolar/lipid raft-mediated endocytosis) were used to perform the cellular uptake tests. The results demonstrated that the selected concentrations had an obvious effect on the blocking endocytosis of corresponding markers (Figure 2B). Meanwhile, phalloidin was used to evaluate the effect of cyto D on disrupting actin polymerization, and the result showed that a 300 nM cyto D exhibited a good inhibitory effect (Figure 2C).

Subsequently, the pseudovirus inhibitory assays were performed and we found that cyto D, nocodazole, filipin III, and MCD significantly inhibit the SARS-CoV-2 pseudovirus infection for Vero E6 cells, while no obvious change was observed in the CPZ and EIPA groups (Figure 3A). These findings indicate that the dominating endocytosis pathways, clathrin-mediated endocytosis, and micropinocytosis are not involved in the infection of SARS-CoV-2 pseudovirus for the host cells. Instead, caveolar/lipid raft- and cytoskeleton-mediated endocytosis might participate or assist in the entry process of SARS-CoV-2. To
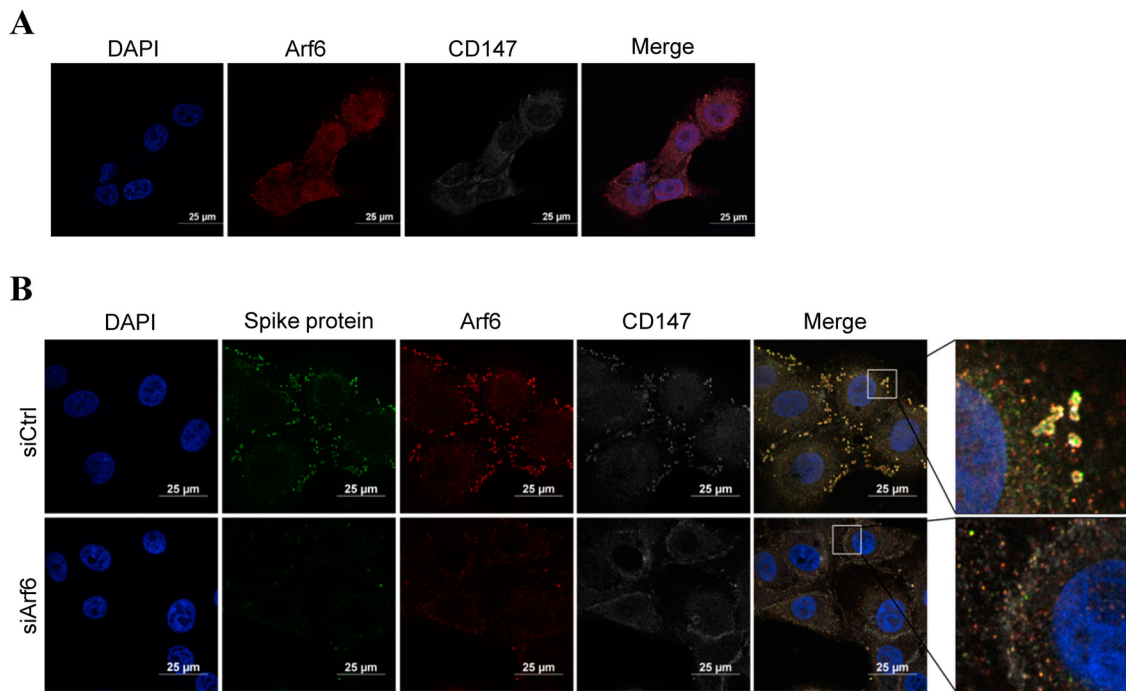
**Figure 4.** The co-localization of targeted proteins was observed by immunofluorescence staining. (A) The co-localization between Arf6 (red) and CD147 (white) was analyzed in Vero E6 cells by immunofluorescence staining. Scale bars, 25 μm. (B) The co-localization of spike protein (green), Arf6 (red), and CD147 (white) was analyzed in Vero E6 cells and Arf6 knockdown cells by multi-colour immunofluorescence staining. Scale bars, 25 μm.

explore the role of CD147 in the screened endocytosis pathways, Vero E6-CD147KO cells were used to perform the pseudovirus inhibitory assays with four inhibitors of MCD, filipin III, cyto D, and nocodazole. Compared to the control group, all four inhibitors reduced SARS-CoV-2 pseudovirus entry in Vero E6-CD147KO cells, which is consistent with the results obtained in Vero E6 cells (Figure 3B). This result indicated that CD147 was not involved in caveolar/lipid raft- and cytoskeleton-dependent endocytosis.

It has been reported that the internalization of CD147 depends on clathrin-independent endocytosis, which is closely related to Arf6 [22,27]. Therefore, we investigated the possible role of Arf6 in CD147-mediated SARS-CoV-2 infection. Arf6 was knocked down in Vero E6 and Huh-7 cells using a specific siRNA, and the silencing efficiency of Arf6 was assessed by RT–PCR (Figure 3C, D). Compared to the control group, Arf6 silencing markedly reduced the infection of pseudovirus (Figure 3C, D), which indicated that Arf6 contributed to the SARS-CoV-2 pseudovirus infection. The expression of ACE2 in the mRNA and protein levels has little change in Arf6 knockdown-Vero E6 cells (Sup. Figure 1E, F). On the contrary, in Vero E6-CD147KO cells, pseudovirus entry was not prevented by silencing Arf6 (Figure 3E). In addition, the co-localization of CD147 (white) and Arf6 (red) was observed in Vero E6 cells by immunofluorescent staining (Figure 4A). We also found the co-localization of spike protein (green), CD147 (white), and Arf6 (red) in Vero E6

cells in the presence of SARS-CoV-2 pseudovirus (Figure 4B). Immunofluorescent staining showed that the knockdown of Arf6 caused the reduction of pseudovirus infection (Figure 4B), which in accordance with the results, was obtained from the luciferase reporter assay. These findings suggest that SARS-CoV-2 pseudovirus enter the host cells through spike protein-CD147 in an Arf6-dependent manner.

## Discussion

The emergence of SARS-CoV-2 and its variants poses an international health emergency. The infection of SASR-CoV-2 depends on the binding of spike protein and receptors on the cell membrane of the host cells. It has been reported that SARS-CoV-2 uses the ACE2 receptor for infection and transmembrane serine protease TMPRSS2 is necessary for spike protein priming, which contributes to ACE2-mediated virus infection [28]. Neuropilin-1 is a novel receptor for SARS-CoV-2 entry, and the antibody against neuropilin-1 attenuates virus infection [29]. AXL is reported to specifically interact with the N-terminal domain of SARS-CoV-2 spike protein, which promotes the infection of pulmonary and bronchial epithelial cells [30]. Our previous study shows that CD147 facilitates virus infection for the host cells by interacting with the SARS-CoV-2 spike protein. Interestingly, sequential endocytosis of SARS-CoV-2 in Vero E6 cells is observed by an electron microscope, and the co-localization of CD147, spike protein, and Rab5 is detected

in the lung tissues of a patient with COVID-19. These results show that SARS-CoV-2 enters the host cells through CD147-mediated endocytosis [13]. In this study, the silencing of CD147 and Rab5a significantly inhibits virus entry, and similar observations from immunofluorescence staining are obtained in Vero E6 cells, which are weakened by CD147 silence. Our findings provide abundant evidence that the SARS-CoV-2 pseudovirus employs CD147 to infect the host cells by endocytosis.

Endocytosis plays a vital role in the infection of numerous viruses. However, the precise endocytic mechanisms for SARS-CoV-2 entry are still unclear. The most common pathways of endocytosis include clathrin-mediated endocytosis, caveolar/lipid raft-mediated endocytosis, macropinocytosis, and cytoskeleton system. Therefore, we first ascertain whether SARS-CoV-2 enters cells through the above routes. In our study, the use of corresponding pharmacological inhibitors has shown that the SARS-CoV-2 infection is not associated with clathrin-mediated endocytosis and macropinocytosis. The treatment with inhibitors of the caveolar/lipid raft and cytoskeleton reduces the infection of SARS-CoV-2 pseudovirus. Therefore, the caveolar/lipid raft and cytoskeleton system may involve or assist in the entry process of SARS-CoV-2 pseudovirus. Lipid rafts enriched in sphingolipids and cholesterol are functional membrane microdomains, which provide a platform to allow receptors such as ACE2, CD147, and TMPRSS2 to be recruited for binding to the viral spike protein [31–34]. A cytoskeleton is composed of three major types of cytoskeletal polymers including actin filaments, microtubules, and intermediate filaments [35]. Dynamic actin rearrangements are crucial for coronavirus entry [36,37]. Therefore, the inhibitors of the caveolar/lipid raft and cytoskeleton system can be used as a potential tool to treat COVID-19.

In our study, we also explored the specific endocytosis type for the CD147-mediated viral infection. A previous study showed that the endocytic recycling of CD147 is closely related to Arf6-mediated endocytosis [27,38]. Arf6-mediated internalization requires the involvement of cholesterol and cytoskeleton, and after internalization, cargo-containing endosomes fuse with Rab5-positive sorting endosomes [8,39,40]. Therefore, we investigate the possible role of Arf6 in CD147-mediated SARS-CoV-2 infection. Immunofluorescence results reveal that CD147, Arf6, and spike protein are co-localized in SARS-CoV-2 pseudovirus-infected Vero E6 cells. The pseudovirus infection assay exhibits that Arf6 silencing significantly inhibits the viral infection in Vero E6 and Huh-7 cells, while little change is observed in CD147 knockout-Vero E6 cells. These results indicate that SARS-CoV-2 pseudovirus entry to the host cells is CD147 receptor-dependent, and the disruption of Arf6-mediated CD147 trafficking inhibits the viral infection. Our study provides a promising patch for treating COVID-19 by targeting CD147 or Arf6.

To sum up, both caveolar/lipid raft- and cytoskeleton-dependent endocytosis contribute to the entry process of SARS-CoV-2 pseudovirus, and Arf6-mediated CD147 endocytosis is required for the infection of SARS-CoV-2 pseudovirus. These findings provide a new insight into the SARS-CoV-2 pseudovirus entry and further suggest that targeting the endocytic pathway of SARS-CoV-2 infection seems to be a potential approach to treat COVID-19.

## References

[1] Tian D, Sun Y, Zhou J, et al. The global epidemic of the SARS-CoV-2 delta variant, key spike mutations and immune escape. Front Immunol. 2021;12:751778.

[2] Ai J, Zhang H, Zhang Y, et al. Omicron variant showed lower neutralizing sensitivity than other SARS-CoV-2 variants to immune sera elicited by vaccines after boost. Emerg Microbes Infect. 2022 Dec:11(1): 337–343.

[3] Sun Y, Tien P. From endocytosis to membrane fusion: emerging roles of dynamin in virus entry. Crit Rev Microbiol. 2013 May;39(2):166–179.

[4] Borkotoky S, Dey D, Banerjee M. Computational insight into the mechanism of SARS-CoV-2 membrane fusion. J Chem Inf Model. 2021 Jan 25;61(1):423–431.

[5] Scialo F, Daniele A, Amato F, et al. ACE2: the major cell entry receptor for SARS-CoV-2. Lung. 2020 Dec;198(6):867–877.

[6] Benton DJ, Wrobel AG, Xu P, et al. Receptor binding and priming of the spike protein of SARS-CoV-2 for membrane fusion. Nature. 2020 Dec;588(7837):327–330.

[7] Xia X. Domains and functions of spike protein in Sars-Cov-2 in the context of vaccine design. Viruses. 2021 Jan 14;13(1):109.

[8] Mercer J, Schelhaas M, Helenius A. Virus entry by endocytosis. Annu Rev Biochem. 2010;79:803–833.

[9] Doherty GJ, McMahon HT. Mechanisms of endocytosis. Annu Rev Biochem. 2009;78:857–902.

[10] Fackler OT, Peterlin BM. Endocytic entry of HIV-1. Curr Biol. 2000 Aug 24;10(16):1005–1008.

[11] Sieczkarski SB, Whittaker GR. Influenza virus can enter and infect cells in the absence of clathrin-mediated endocytosis. J Virol. 2002 Oct;76 (20):10455–10464.

[12] Nunes-Correia I, Eulálio A, Nir S, et al. Caveolae as an additional route for influenza virus endocytosis in MDCK cells. Cell Mol Biol Lett. 2004;9(1):47–60.

[13] Wang K, Chen W, Zhang Z, et al. CD147-spike protein is a novel route for SARS-CoV-2 infection to host cells. Signal Trans Targ Ther. 2020 Dec 4;5 (1):283.

[14] Muramatsu T. Basigin: a multifunctional membrane protein with an emerging role in infections by malaria parasites. Expert Opin Ther Targets. 2012 Oct;16 (10):999–1011.

[15] Iacono KT, Brown AL, Greene MI, et al. CD147 immunoglobulin superfamily receptor function and role in pathology. Exp Mol Pathol. 2007 Dec;83 (3):283–295.

[16] Jiang JL, Zhou Q, Yu MK, et al. The involvement of HAb18G/CD147 in regulation of store-operated calcium entry and metastasis of human hepatoma cells. J Biol Chem. 2001 Dec 14;276(50):46870–7.

[17] Wang K, Huang W, Chen R, et al. Di-methylation of CD147-K234 promotes the progression of NSCLC by enhancing lactate export. Cell Metab. 2021 Jan 5;33(1):160–173.e6.

[18] Chen Y, Xu J, Wu X, et al. CD147 regulates antitumor CD8(+) T-cell responses to facilitate tumor-immune escape. Cell Mol Immunol. 2021 Aug;18(8):1995–2009.

[19] Geng J, Chen R, Yang FF, et al. CD98-induced CD147 signaling stabilizes the Foxp3 protein to maintain tissue homeostasis. Cell Mol Immunol. 2021 Dec;18 (12):2618–2631.

[20] Zhang MY, Zhang Y, Wu XD, et al. Disrupting CD147-RAP2 interaction abrogates erythrocyte invasion by plasmodium falciparum. Blood. 2018 Mar 8;131(10):1111–1121.

[21] Pushkarsky T, Zybarth G, Dubrovsky L, et al. CD147 facilitates HIV-1 infection by interacting with virus-associated cyclophilin A. Proc Natl Acad Sci USA. 2001 May 22;98(11):6360–6365.

[22] Qi S, Su L, Li J, et al. Arf6-driven endocytic recycling of CD147 determines HCC malignant phenotypes. J Exp Clin Cancer Res. 2019 Nov 21;38(1):471.

[23] Nie J, Li Q, Wu J, et al. Establishment and validation of a pseudovirus neutralization assay for SARS-CoV-2. Emerg Microbes Infect. 2020 Dec;9 (1):680–686.

[24] Zerial M, McBride H. Rab proteins as membrane organizers. Nat Rev Mol Cell Biol. 2001 Feb;2(2):107–117.

[25] Feliciano WD, Yoshida S, Straight SW, et al. Coordination of the Rab5 cycle on macropinosomes. Traffic. 2011 Dec;12(12):1911–1922.

[26] Zerial M. Regulation of endocytosis by the small GTP-ase rab5. Cytotechnology. 1993;11(Suppl 1): S47–S49.

[27] Eyster CA, Higginson JD, Huebner R, et al. Discovery of new cargo proteins that enter cells through clathrin-independent endocytosis. Traffic. 2009 May;10 (5):590–599.

[28] Hoffmann M, Kleine-Weber H, Schroeder S, et al. SARS-CoV-2 cell entry depends on ACE2 and TMPRSS2 and is blocked by a clinically proven protease inhibitor. Cell. 2020 Apr 16;181(2):271–280.e8.

[29] Cantuti-Castelvetri L, Ojha R, Pedro LD, et al. Neuropilin-1 facilitates SARS-CoV-2 cell entry and infectivity. Science (New York. NY). 2020 Nov 13;370(6518):856–860.

[30] Wang S, Qiu Z, Hou Y, et al. AXL is a candidate receptor for SARS-CoV-2 that promotes infection of pulmonary and bronchial epithelial cells. Cell Res. 2021 Feb;31(2):126–140.

[31] Palacios-Rápalo SN, De Jesús-González LA, Cordero-Rivera CD, et al. Cholesterol-rich lipid rafts as platforms for SARS-CoV-2 entry. Front Immunol. 2021;12:796855.

[32] Suzuki T, Suzuki Y. Virus infection and lipid rafts. Biol Pharm Bull. 2006 Aug;29(8):1538–1541.

[33] Li GM, Li YG, Yamate M, et al. Lipid rafts play an important role in the early stage of severe acute respiratory syndrome-coronavirus life cycle. Microbes Infect. 2007 Jan;9(1):96–102.

[34] Lu Y, Liu DX, Tam JP. Lipid rafts are involved in SARS-CoV entry into Vero E6 cells. Biochem Biophys Res Commun. 2008 May 2;369(2):344–349.

[35] Fletcher DA, Mullins RD. Cell mechanics and the cytoskeleton. Nature. 2010 Jan 28;463(7280):485–492.

[36] Milewska A, Nowak P, Owczarek K, et al. Entry of human coronavirus NL63 into the cell. J Virol. 2018 Jan 17;92(3):e01933-17.

[37] Owczarek K, Szczepanski A, Milewska A, et al. Early events during human coronavirus OC43 entry to the cell. Sci Rep. 2018 May 8;8(1):7124.

[38] Maldonado-Baez L, Williamson C, Donaldson JG. Clathrin-independent endocytosis: a cargo-centric view. Exp Cell Res. 2013 Nov 1;319(18):2759–2769.

[39] Naslavsky N, Weigert R, Donaldson JG. Convergence of non-clathrin- and clathrin-derived endosomes involves Arf6 inactivation and changes in phosphoinositides. Mol Biol Cell. 2003 Feb;14(2):417–431.

[40] Mayor S, Parton RG, Donaldson JG. Clathrin-independent pathways of endocytosis. Cold Spring Harbor Perspect Biol. 2014 Jun 2;6(6):a016758.